THYROID
Volume 21, Number 9, 2011

DOI: 10.1089/thy.2011.0030

Establishment and Characterization of Cell Lines from a Novel Mouse Model of Poorly Differentiated Thyroid Carcinoma: Powerful Tools for Basic and Preclinical Research

Mariavittoria Dima,[1,*] Kelly A. Miller,[2,*] Valeria Gabriela Antico-Arciuch,[1] and Antonio Di Cristofano[1,2]

Background: Poorly differentiated and anaplastic thyroid carcinomas have a rather poor prognosis. The development of relevant model systems to unravel *in vitro* and *in vivo* the molecular mechanisms governing the resistance of these tumors to therapy, as well as to test novel drug combinations, is a clear priority for thyroid-focused research.
Methods: Several novel cell lines were established from tumors developed by mice engineered to simultaneously express a loss-of-function *Pten* allele and an oncogenic *Kras* allele.
Results: Similar to most poorly differentiated thyroid tumors, these cell lines are characterized by simultaneous activation of the PI3K and MAPK pathways, by the presence of wild-type, functional p53, and by the severe downregulation of thyroid differentiation markers, including sodium-iodide symporter (NIS). Further, they display a highly glycolytic phenotype. They can be grafted to syngeneic, immunocompetent hosts, and easily metastasize to the lungs.
Conclusions: These mouse cell lines are a novel and invaluable tool that can be used to develop innovative therapeutic approaches to poorly differentiated carcinomas in a more physiological context than using xenografts of human cell lines in immunocompromised mice.

Introduction

The thyroid is the most frequent site of endocrine malignancy (1). While well-differentiated thyroid cancer usually has a favorable prognosis, poorly differentiated and undifferentiated tumors account for over 50% of deaths for thyroid cancer due to the limited therapeutic options available (2–4). The development of relevant models for basic and preclinical research is thus a key step toward a rationale testing of novel therapeutic approaches. Cell lines derived from human thyroid tumors are available (although recent data have questioned the identity and origin of many of them) and have been successfully used to test the efficacy of novel drugs and drug combinations. However, they have the disadvantage of limiting preclinical studies to the tissue culture setting, or to xenografts in immunocompromised mice, precluding the ability to take into account the interactions between the growing tumor and the host immune system.

Cell lines established from tumors developed by genetically engineered mouse models, in contrast, can be grown in syngeneic immunocompetent hosts, implanted subcutaneously or as orthotopic implants, and thus offer the opportunity to analyze tumor behavior and drug response in a physiological setting (5,6).

We have recently described a mouse model of follicular carcinoma based on the simultaneous inactivation of the *Pten* tumor suppressor gene and the activation of the *Kras* G12D oncogenic allele from its endogenous locus (7). These compound mutants develop, within 8 weeks from birth, follicular neoplastic lesions often containing areas of poorly differentiated carcinomas.

Here we describe the establishment and characterization of several thyroid cancer cell lines derived from primary tumors developed by $Pten^{-/-};Kras^{G12D}$ compound mutants.

Materials and Methods

Mouse model

The $Pten^{-/-};Kras^{G12D}$ strain has been described (7). All mice were backcrossed into the 129Sv background for at least eight generations.

[1]Department of Developmental and Molecular Biology, Albert Einstein College of Medicine, Bronx, New York.
[2]Human Genetics Program, Fox Chase Cancer Center, Philadelphia, Pennsylvania.
*These authors equally contributed to this work.

Establishment and maintenance of cell lines

Primary thyroids and tumors were minced and resuspended in Ham's F12/10% fetal bovine serum (FBS) with 100 U/mL type I collagenase (Sigma, St. Louis, MO) and 1 U/mL dispase (Roche, Indianapolis, IN). Enzymatic digestion was carried out for 90 minutes at 37°C. After digestion, cells were seeded in Ham's F12 containing 40% Nu-Serum IV (Collaborative Biomedical, Bedford, MA), gly-his-lys (10 ng/mL; Sigma), and somatostatin (10 ng/mL; Sigma) and allowed to spread and reach confluence before being passaged. After the fourth passage, tumor cells were adapted to grow in Dulbecco's modified Eagle's medium/10% FBS.

Karyotyping

Metaphase spreads and G-banding were prepared using standard procedures. Chromosome identification and karyotype designations were in accordance with University of Washington guidelines available at www.pathology.washington.edu/research/cytopages/idiograms/mouse

Mutation detection

Genomic DNA was isolated from the established cell lines and subjected to polymerase chain reaction (PCR) to amplify fragments suitable for sequencing. Primer sequences are presented in Supplementary Table S1 (Supplementary Data are available online at www.liebertonline.com/thy). PCR products were gel purified and sequenced from both ends.

Real-time PCR

Total RNA was extracted with Trizol and reverse transcribed using the Thermoscript kit (Invitrogen, Carlsbad, CA). quantitative reverse transcription polymerase chain reaction (qRT-PCR) was performed on a StepOne Plus apparatus using the Absolute Blue qPCR Rox Mix (Thermo Scientific, Waltham, MA) and TaqMan expression assays (Applied Biosystems, Carlsbad, CA). Each sample was run in triplicate and *GusB* was used to control for input RNA. Data analysis was based on the Ct method, and experiments were repeated at least three times.

Western blotting

Cells were lysed on ice in RIPA buffer supplemented with Complete protease inhibitor tablet (Roche). Western blot analysis was carried out on 20–40 μg proteins with the following antibodies: p53, mdm2, p21 (all from Santa Cruz Biotechnology, Santa Cruz, CA), and beta actin (Sigma).

Lactate assay

Twenty-four hours after seeding, cells were washed and culture medium was replaced. Lactate levels were assayed in the supernatant at different time points using a commercially available kit (Biovision, Mountain View, CA). Lactate levels were normalized to the amount of DNA extracted from each well.

Growth curves

Pharmacological inhibitors of PI3K (LY294002, 30 μM), mTOR (RAD001, 50 nM), MEK1 (PD98059, 50 μM), and glycolysis (3-Bromopyruvate, 10–120 μM) were added 24 hours after plating, in quadruplicate. At the indicated time points, cells were trypsinized and counted using a Beckman Coulter counter.

Growth in syngeneic hosts

About 10^7 cells in PBS were injected into the flank of sex-matched wild-type 129Sv mice. Mice were sacrificed 4 weeks after injection for tumor removal and analysis.

Luciferase-expressing lines

T826 cells were infected with a retrovirus encoding luciferase, selected in hygromycin, and injected (1×10^6 cells) into the thyroid bed of wild-type mice. For biophotonic imaging on the IVIS Spectrum (Caliper Life Sciences, Hopkinton, MA),

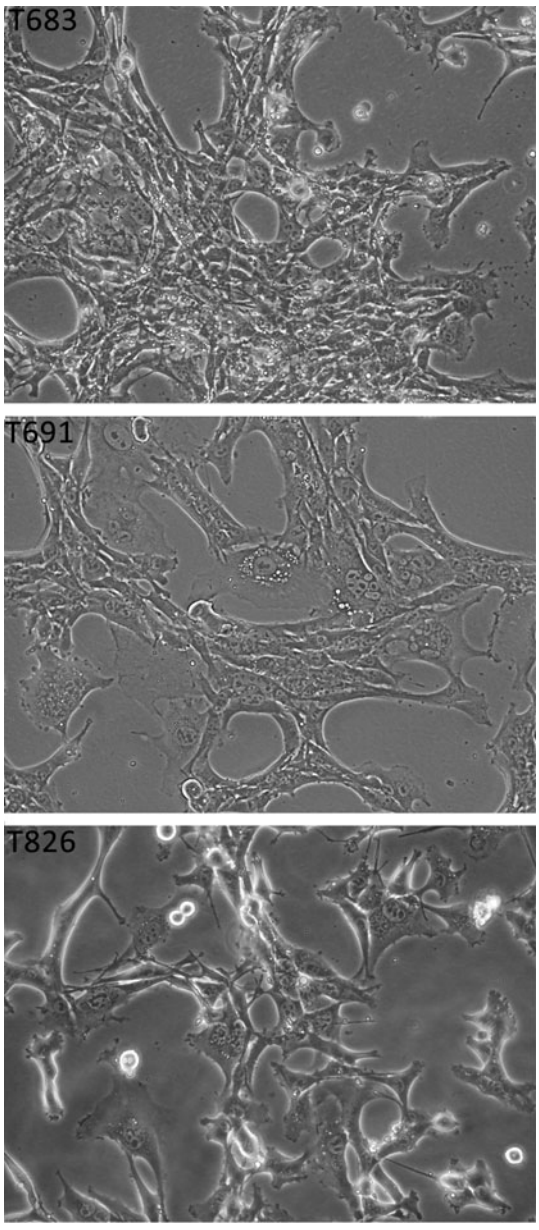

FIG. 1. Morphological features of the T683, T691, and T826 cell lines. Phase-contrast photomicrographs were taken at 200× magnification.

1% isoflurane/oxygen-anesthetized mice were injected with luciferin (4 mg/animal) into the i.p. cavity.

Statistical analysis

Experiments were performed at least three times. Data were analyzed using the JMP 5.1 and Prism software packages. Differences with p-values <0.05 were considered statistically significant.

Results

Several poorly differentiated follicular carcinomas developing in $Pten^{-/-}$;$Kras^{G12D}$ compound mutants were enzymatically dissociated and plated in thyroid-supportive medium (8). After four to six passages, homogeneous populations had taken over the cultures and were gradually adapted to grow in Dulbecco's modified Eagle's medium supplemented with 10% FBS. Three of these lines (T683, T826, and T691) were chosen for complete genetic and molecular characterization. These cells grow as monolayers of epithelial polygonal cells with large and round nuclei containing several nucleoli (Fig. 1).

PCR analysis using primer pairs specific for the *Pten* and *Kras* wild-type, *floxed*, and recombined alleles was carried out to demonstrate that the established cell lines had undergone correct recombination at both loci, thus constitutively activating the PI3K and MAPK pathways (7) (Fig. 2A). As expected, the cell lines had completely lost the floxed Pten

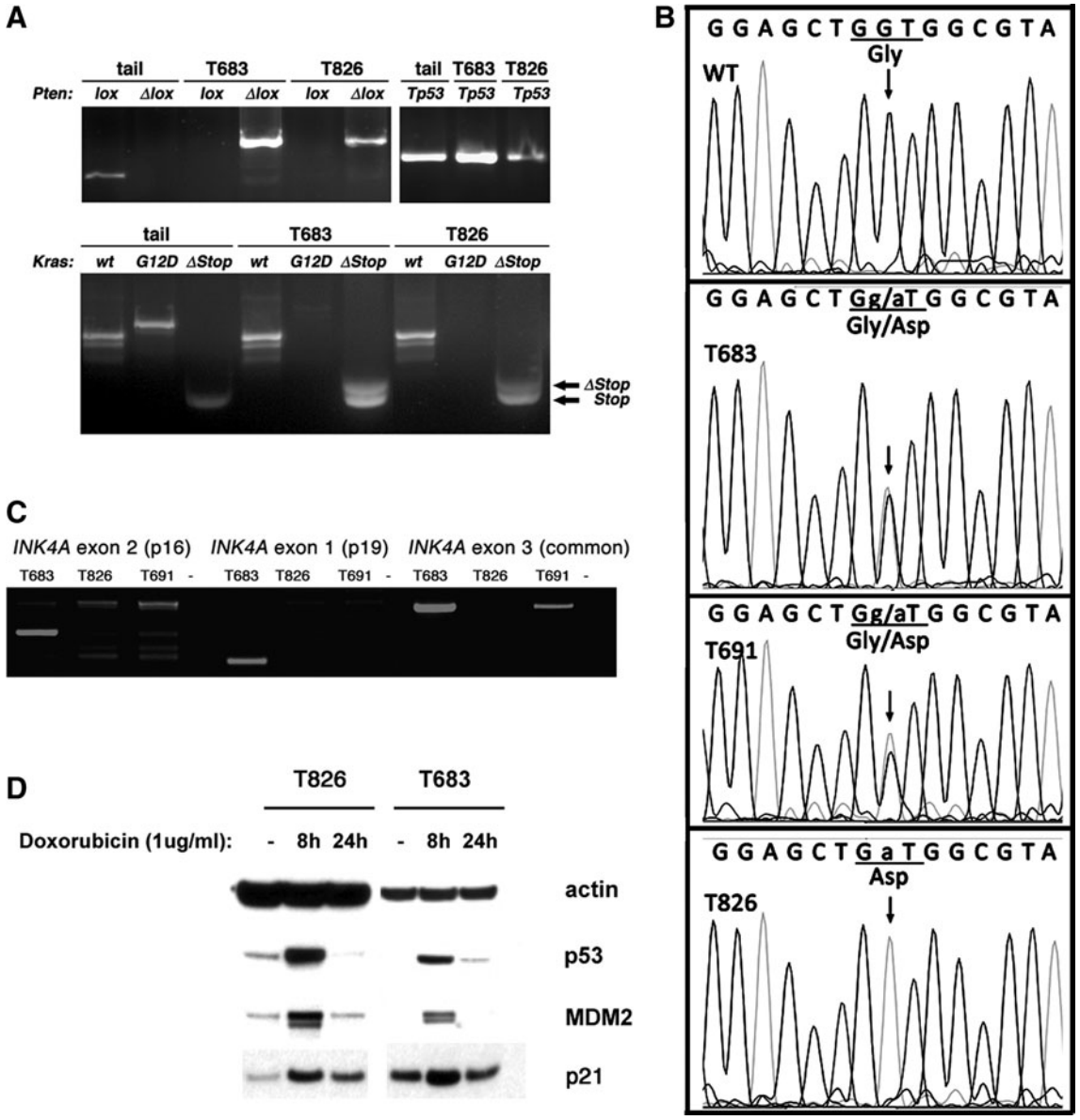

FIG. 2. Genetic features of the T683 and T826 cell lines. **(A)** Polymerase chain reaction (PCR) analysis of control tail DNA and cell line DNA, showing specific deletion of *Pten* (Δlox band), and activation of the $Kras^{G12D}$ allele (ΔStop band). *Tp53* amplification is shown as a control of DNA quality. Same results were obtained for the T691 cell line. **(B)** Electropherograms showing the presence of the $Kras^{G12D}$ allele (Gly to Asp conversion). **(C)** Exon-specific PCR analysis of the *Ink4a* locus, showing locus integrity in T683, and deletion in T826 (all three exons) and T961 (exons 1 and 2). **(D)** Western blotting analysis showing normal p53-mediated response to DNA damage in T683 and T826 cells. Similar results were obtained in T691.

Table 1. Karyotype Analysis of the T683, T691, and T826 Cell Lines

Cell line	Modal chromosome number	Karyotype
T683	40	40, XY, der(4)t(4;10)(E2;B5.2) [17]
T691	40	40, XY, del(4)(C4), dic(12;18) + 18 [20]
T826	40	40, XY [19]

alleles, and had deleted the STOP cassette that prevented $Kras^{G12D}$ expression.

To further confirm that the cell lines were carrying the G12D activating mutation, we PCR amplified and sequenced *Kras* exon 1. Surprisingly, while the T683 and T691 cell lines had the expected heterozygous configuration, we found that the T826 cells have become homozygous for the *G12D* allele (Fig. 2B). Sequence analysis showed that nearby restriction sites specific to the mutant allele were also in a homozygous configuration, suggesting that either the wild-type allele has been completely lost, or it has been replaced by a mutant allele through recombination, rather than becoming a G12D allele through a point mutation.

Karyotype analysis revealed that all three lines have a normal chromosome number (Table 1). However, both the T683 and the T691 lines have chromosome 4 rearrangements, affecting different chromosomal regions.

To determine whether other relevant genes commonly mutated or lost during thyroid tumor progression are affected in these cell lines, we first performed PCR on genomic DNA from these cells with primers specific for the three exons of the *Ink4a* locus, encoding the two tumor suppressors, p16 and p19ARF (Fig. 2C). While the T683 line showed the correct amplification products for all three exons, the results for the T826 line suggest a homozygous deletion affecting the whole locus, whereas the T691 line has lost both exons 1 and 2. Thus, in both cell lines, expression of p16 and p19ARF is completely lost.

We next sought to determine whether p53 is functional in these cells. Thus, we treated the thyroid cancer cell lines with Doxorubicin for 8 and 24 hours to induce DNA damage response, and tested the induction of p53 itself and its targets,

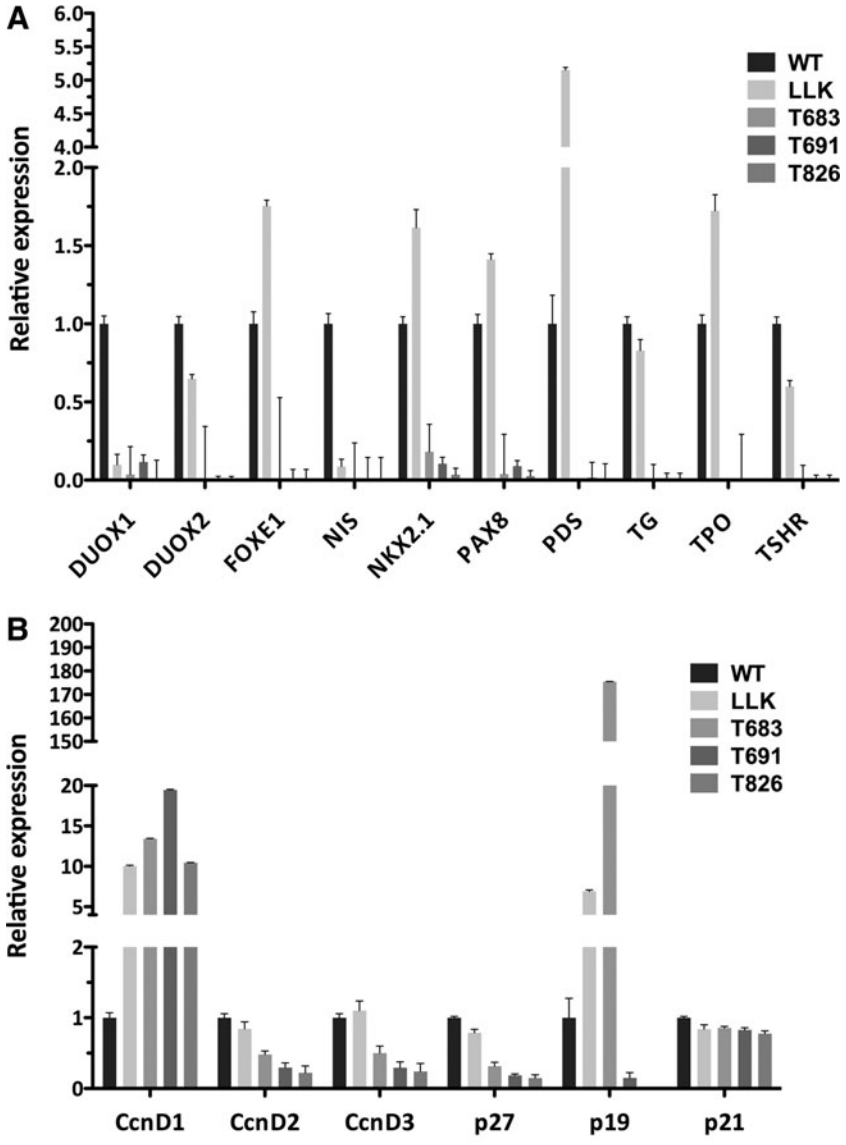

FIG. 3. Real-time PCR analysis of the expression levels of thyroid differentiation markers **(A)** and cell cycle regulators **(B)**. RNA from a primary $Pten^{-/-}$; $Kras^{G12D}$ preneoplastic thyroid (LLK) is included as a control.

p21 and mdm2, by Western blot (Fig. 2D). In all three cell lines (T691 not shown in Fig. 2D) these proteins were induced as expected, strongly suggesting that p53 is intact and functional.

Finally, we PCR amplified and sequenced the Hras, Nras, and Braf exons most commonly mutated in human tumors (exons 1 and 2 for the Ras isoforms, and exons 11 and 15 for Braf). No mutations were identified in any of these locations (data not shown), strongly suggesting that these three genes do not contribute to the transformed phenotype exhibited by the T683, T826, and T691 thyroid carcinoma cell lines.

We measured by real-time PCR the mRNA levels of a panel of genes involved in thyroid differentiation and function (*Foxe1*, *Nkx2-1*, *Pax8*, *Duox1* and *-2*, *Nis*, *Pds*, *TG*, *Tpo*, and *Tshr*) and found that expression of these genes is virtually abolished in all three lines, confirming that these cells are a relevant model of undifferentiated and poorly differentiated thyroid tumors (Fig. 3A). Quantitative PCR was also utilized to determine the expression levels of genes involved in cell cycle control and proliferation. We found that expression of *Cyclin D1*, but not *D2* or *D3*, was strikingly increased in all three lines. *p27* expression was drastically reduced in all lines, whereas *p19ARF* was dramatically upregulated in T683 (the only line with an intact *Ink4a* locus). Finally, *p21* was not deregulated in any of the three cell lines (Fig. 3B).

To evaluate the effect of pathway-specific inhibitors on the proliferation of these cells, we generated growth curves in the presence of LY294002 (PI3K inhibitor), RAD001 (mTOR inhibitor), and PD98059 (MEK inhibitor). In all lines, mTOR or MEK inhibition, alone, was only partially effective (Fig. 4A, B). PI3K inhibition had a cytostatic effect, as had the combination of mTOR and MEK inhibitors. Simultaneous inhibition of both PI3K and MEK was instead able to induce cell death and effectively reduce cell number (Fig. 4A, B).

Many tumors display a switch from an oxidative phosphorylation energy production mode to a glycolytic mode (Warburg effect), and PI3K activation contributes to this metabolic switch through different mechanisms (9,10). Thus, we compared lactate production, an index of glycolytic metabolism, in primary wild-type thyrocytes and in the T683 cells. T683 produced lactate with a much higher kinetics than control thyrocytes (Fig. 4C), strongly suggesting that these cells display the Warburg effect.

Next, we tested whether glycolysis inhibition would be effective as a therapeutic approach. Indeed, cell growth was

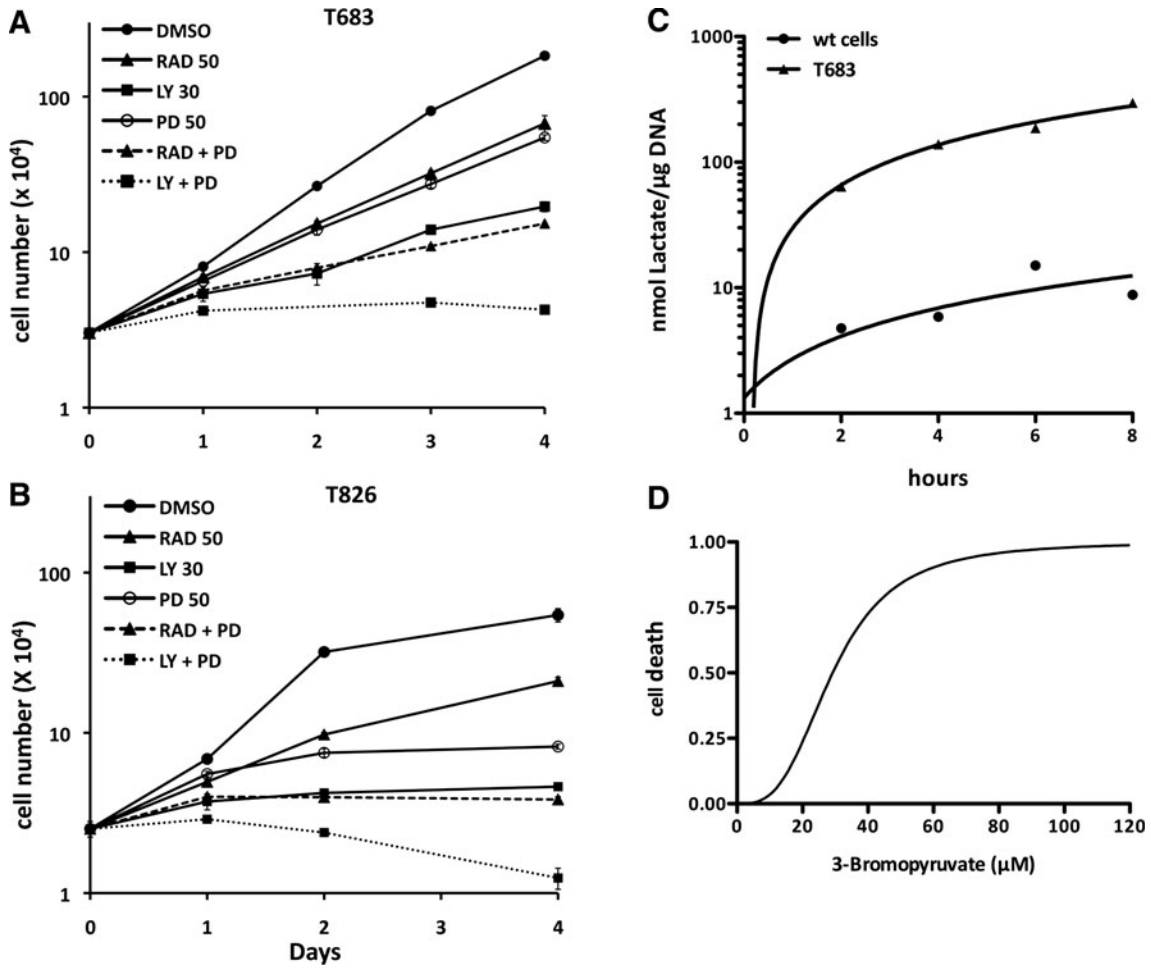

FIG. 4. **(A, B)** Growth suppressive effect of pathway-specific inhibitors in the T683 and T826 cell lines. RAD: RAD001, LY: LY294002, PD: PD98059. **(C)** Kinetics of lactate production in wild-type primary thyrocytes and T683 cells. **(D)** Dose-dependent response of T683 cells to the glycolysis inhibitor 3-bromopyruvate.

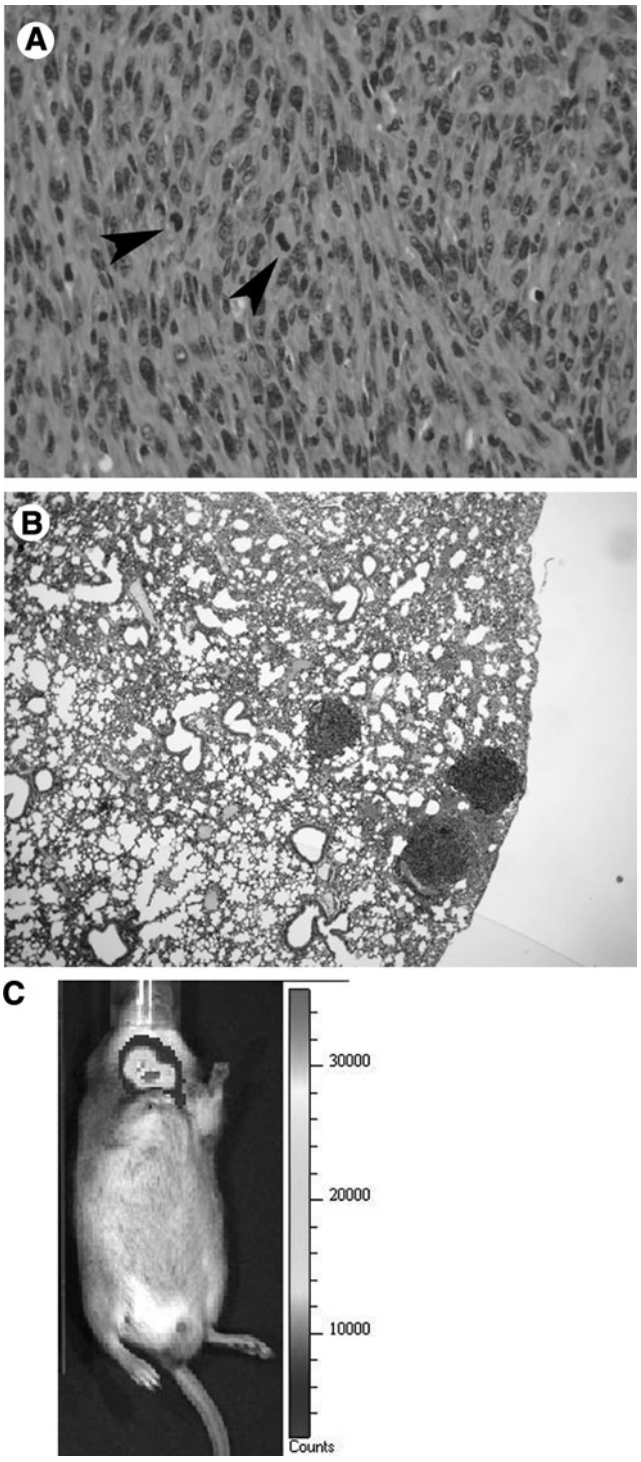

FIG. 5. Tumor development in syngeneic mice. **(A)** H&E showing poorly differentiated cells with several mitotic figures (arrowheads). **(B)** Multiple lung metastases developing in the injected mice. **(C)** IVIS analysis showing luciferase expression after injection of engineered T826 cells into the thyroid bed. Original magnification: 200× **(A)**, 40× **(B)**.

inhibited in a dose-dependent manner by the Hexokinase inhibitor, 3-Bromopyruvate (11) (Fig. 4D).

Finally, we tested the ability of these cells to grow in syngeneic, immunocompetent hosts. About 10^7 cells were subcutaneously injected in the flank of wild-type 129Sv mice, and recipients were followed up for 4 weeks. At this time point, tumor size had exceeded 2 cm and the injected mice were sacrificed for histopathologycal analysis. Tumors were composed of spindle-like cells exhibiting frequent mitotic figures (Fig. 5A). Further, they had metastasized to the lungs (Fig. 5B). Thus, these cells can be an invaluable tool for preclinical studies in immunocompetent hosts.

To establish a system in which tumor progression can be observed *in vivo*, T826 cells were engineered to express the luciferase reporter and implanted into the thyroid bed of syngeneic mice. One week after implantation, luciferase activity was readily detected in the neck area of the injected mice (Fig. 5C).

Discussion and Conclusions

Cell lines derived from tumor developing in genetically engineered mice are an invaluable tool for both basic and preclinical research. On one hand, they allow us to study pathways and networks altered as a consequence of specific, clinically relevant genetic alterations; on the other, they can be implanted in immunocompetent mice, thus permitting the analysis of the interactions between the growing tumor and the host immune system, the metastatic process, and the response to therapy in a physiological setting.

We have generated and characterized three novel cell lines having simultaneous activation of PI3K and MAPK signaling, a combination often found in poorly differentiated thyroid tumors (12).

These lines display a normal chromosome number, differ in their *Ink4a* genomic status, and do not harbor mutations in *p53* and *Braf*. Similar to many aggressive tumors and tumor cell lines, they have a prominent glycolytic phenotype and can be targeted by glycolysis inhibitors.

They have drastically reduced expression of most thyroid differentiation markers, including sodium-iodide symporter (NIS), to an extent superior to that of the original tumors (compare $Pten^{-/-};Kras^{G12D}$ expression levels to that in the cell lines in Fig. 3A), and readily grow in syngeneic (129Sv) hosts when implanted either on the flank or in the thyroid bed, giving rise to poorly differentiated and anaplastic tumors. The increased aggressiveness of the implanted tumors compared to the original lesions underlines the acquisition of still undetermined additional genetic changes, which may likely recapitulate the genetic complexity of human advanced thyroid carcinomas.

Finally, luciferase-expressing cells allow for noninvasive, longitudinal studies of tumor response to targeted therapies.

It is thus clear that these cells represent a novel, clinically relevant model to develop therapies targeting poorly differentiated and undifferentiated thyroid tumors, both in the tissue culture setting and *in vivo*.

Acknowledgments

The authors acknowledge the Animal Facility and the Genomic Facility of the Einstein College of Medicine, and the Cytogenetics and Imaging Facilities of Fox Chase Cancer Center. We also thank M. E. Murphy (FCCC) for the generous gift of luciferase-encoding retroviral constructs. This work was supported by the AECC Core Grant, and by NIH grants to ADC (CA97097 and CA128943).

Disclosure Statement

The authors declare that no competing financial interests exist.

References

1. Davies L, Welch HG 2006 Increasing incidence of thyroid cancer in the United States, 1973–2002. JAMA **295:**2164–2167.
2. Wein RO, Weber RS 2011 Anaplastic thyroid carcinoma: palliation or treatment? Curr Opin Otolaryngol Head Neck Surg DOI: 10.1002/mc.20668.
3. Asioli S, Erickson LA, Righi A, Jin L, Volante M, Jenkins S, Papotti M, Bussolati G, Lloyd RV 2010 Poorly differentiated carcinoma of the thyroid: validation of the Turin proposal and analysis of IMP3 expression. Mod Pathol **23:**1269–1278.
4. Patel KN, Shaha AR 2006 Poorly differentiated and anaplastic thyroid cancer. Cancer Control **13:**119–128.
5. Shan YS, Fang JH, Lai MD, Yen MC, Lin PW, Hsu HP, Lin CY, Chen YL 2010 Establishment of an orthotopic transplantable gastric cancer animal model for studying the immunological effects of new cancer therapeutic modules. Mol Carcinog DOI: 10.1097/moo.0b013e3283432f3d.
6. Quinn BA, Xiao F, Bickel L, Martin L, Hua X, Klein-Szanto A, Connolly DC 2010 Development of a syngeneic mouse model of epithelial ovarian cancer. J Ovarian Res **3:**24–40.
7. Miller KA, Yeager N, Baker K, Liao XH, Refetoff S, Di Cristofano A 2009 Oncogenic Kras requires simultaneous PI3K signaling to induce ERK activation and transform thyroid epithelial cells *in vivo*. Cancer Res **69:**3689–3694.
8. Jeker LT, Hejazi M, Burek CL, Rose NR, Caturegli P 1999 Mouse thyroid primary culture. Biochem Biophys Res Commun **257:**511–515.
9. Dang CV, Semenza GL 1999 Oncogenic alterations of metabolism. Trends Biochem Sci **24:**68–72.
10. Wallace DC 2005 Mitochondria and cancer: Warburg addressed. Cold Spring Harb Symp Quant Biol **70:**363–374.
11. Ko YH, Smith BL, Wang Y, Pomper MG, Rini DA, Torbenson MS, Hullihen J, Pedersen PL 2004 Advanced cancers: eradication in all cases using 3-bromopyruvate therapy to deplete ATP. Biochem Biophys Res Commun **324:**269–275.
12. Liu Z, Hou P, Ji M, Guan H, Studeman K, Jensen K, Vasko V, El-Naggar AK, Xing M 2008 Highly prevalent genetic alterations in receptor tyrosine kinases and phosphatidylinositol 3-kinase/akt and mitogen-activated protein kinase pathways in anaplastic and follicular thyroid cancers. J Clin Endocrinol Metab **93:**3106–3116.

Address correspondence to:
Antonio Di Cristofano, Ph.D.
Department of Developmental and Molecular Biology
Albert Einstein College of Medicine
1301 Morris Park Ave., Room 302
Bronx, NY 10461

E-mail: antonio.dicristofano@einstein.yu.edu